

# Osteogenic properties of calcium phosphate ceramics and fibrin glue based composites

Damien Le Nihouannen · Afchine Saffarzadeh · Eric Aguado · Eric Goyenvalle · Olivier Gauthier · Françoise Moreau · Paul Pilet · Reiner Spaethe · Guy Daculsi · Pierre Layrolle

Received: 19 June 2006 / Accepted: 23 August 2006  
© Springer Science + Business Media, LLC 2007

**Abstract** Calcium phosphate (Ca-P) ceramics are currently used in various types of orthopaedic and maxillofacial applications because of their osteoconductive properties. Fibrin glue is also used in surgery due to its haemostatic, chemotactic and mitogenic properties and also as scaffolds for cell culture and transplantation. In order to adapt to surgical sites, bioceramics are shaped in blocks or granules and preferably in porous forms. Combining these bioceramics with fibrin glue provides a mouldable and self-hardening composite biomaterial. The aim of this work is to study the osteogenic properties of this composite material using two different animal models. The formation of newly formed bone (osteinduction) and bone healing capacity (osteconduction) have been studied in the paravertebral muscles of sheep and in critical sized defects in the femoral condyle of rabbits, respectively. The different implantation sites were filled with composite material associating Ca-P granules and fibrin glue. Ca-P granules of 1–2 mm were composed with 60% of hydroxyapatite and 40% of beta tricalcium phosphate in weight. The fibrin glue was composed of fibrinogen, thrombin and other

biological factors. After both intramuscular or intraosseous implantations for 24 weeks and 3, 6, 12 and 24 weeks, samples were analyzed using histology and histomorphometry and mechanical test. In all cases, the newly formed bone was observed in close contact and around the ceramic granules. Depending on method of quantification, 6.7% (with BSEM) or 17% (with  $\mu$ CT) of bone had formed in the sheep muscles and around 40% in the critical sized bone rabbit defect after 24 weeks. The Ca-P/fibrin material could be used for filling bone cavities in various clinical indications.

## 1 Introduction

It is estimated that, every year, more than one million patients worldwide need bone graft surgery [1]. For the reconstruction of large skeletal defects, autologous bone graft is the gold standard because it combines osteogenic, osteoinductive and osteoconductive properties [2]. However, autograft is often associated with complications at the harvesting site and limited in quantity [3, 4]. Bone allografts are less osteogenic, more immunogenic and have a greater rate of resorption than autologous bone grafts [5]. In addition, disease transmissions (e.g. HIV, hepatitis) have been reported [6].

During the last decade, calcium phosphate ceramics have been widely used as an alternative to these biological grafts in various types of bone surgery [7]. These synthetic materials have shown good results in many clinical applications. In fact, bioceramics made of hydroxyapatite, beta tricalcium phosphate and mixtures have demonstrated bioactivity and osteoconductivity [8]. For specific clinical indications, bioceramics blocks could be shaped to the surgical site. However, calcium phosphate ceramic granules are generally preferred for filling bone defects but they are difficult to handle and to maintain in the surgical sites leading to a lot of empty spaces

---

D. Le Nihouannen (✉) · A. Saffarzadeh · O. Gauthier · F. Moreau · P. Pilet · G. Daculsi · P. Layrolle  
Inserm, U791, Nantes, France, Laboratoire d'ingénierie ostéoarticulaire et dentaire; Univ. Nantes, Faculté de chirurgie dentaire, 1 place Alexis Ricordeau, F-44042 Nantes, France  
e-mail: damien.lenihouannen@mcgill.ca

E. Aguado · E. Goyenvalle · O. Gauthier  
Ecole Nationale Vétérinaire de Nantes, Service de chirurgie, route de Gachet, 44307 Nantes, France

P. Pilet  
Inserm RIO IFR 26-1, place Alexis Ricordeau, 44042 Nantes, France

R. Spaethe  
Baxter BioSciences BioSurgery, Vienna, Austria

between the granules and bone tissue with a mechanical instability. In spite of their osteoconductive properties, calcium phosphate ceramic granules generally lack osteogenic properties for the regeneration of mineralized tissue into critical sized bone defects. Certain calcium phosphate bioceramics have recently been shown to induce ectopic bone formation [9–11]. The biological mechanism leading to osteoinduction by biomaterials has not yet been identified and several hypotheses have been proposed [8, 12].

Fibrin sealants derived from human blood plasma have been used in various surgeries (abdominal, thoracic, vascular, oral, endoscopic) due to their wound healing, tissue adhesion and blood clotting properties [13, 14]. Fibrin glues mimic the last step of the coagulation cascade through activation of fibrinogen by thrombin, resulting in a clot of fibrin with adhesive properties. Fibrin glues could also be used as scaffolds for cell culture and transplantation due to their biocompatibility, biological degradation and cell attraction properties [15]. Only a few publications have reported the osteoinductive properties of fibrin glue and these properties are subjected to controversy [17, 18].

In the context of bone reconstruction, the association of the calcium phosphate ceramic granules to a binding agent such as fibrin glue may produce an easy-shaped composite material without empty spaces [16]. The initial mechanical stability of the composite material may be achieved through its adaptation and adhesion to the walls of the bone defect. Nevertheless, the association between calcium phosphate granules and a regenerative binding agent such as fibrin sealants has not yet demonstrated osteogenic properties for regenerating large bone defects. In this prospect, the extracorporeal association of fibrin sealant, biphasic calcium phosphate ceramic granules may produce an interesting alternative to autologous or allogeneous bone grafts [19–23].

In this study, we aim to investigate the osteogenic and mechanical properties of macro-/micro-porous biphasic calcium phosphate (MBCP) ceramic granules associated with fibrin glue. MBCP granules were mixed with fibrin glue following two procedures. The fibrin sealant was prepared by either simultaneous or sequential mixing of the components. Several publications have already shown the important role of thrombin in the formation of MBCP granule/fibrin composite materials but also onto the bone cell biology [24, 25]. Adsorption, at first, of thrombin onto the MBCP granules could result in a modification of the properties of the hybrid/composite material. Composite materials were implanted into the paravertebral muscles of sheep and into critical sized defects of rabbit's femoral condyle for 3, 6, 12 and 24 weeks. After explantation, the samples were analyzed using histology, histomorphometry and micro-indentation. The mechanical and biological properties of newly formed bone were compared.

## 2 Materials and methods

### 2.1 Preparation and characterization of materials

Micro- macro- porous biphasic calcium phosphate granules (MBCP, TricOs<sup>®</sup>, Baxter BioSciences BioSurgery, Vienna, Austria; Biomatlante, France, Manufacturer) measuring 1–2 mm in diameter were used. The MBCP granules were prepared by mixing calcium-deficient apatite with pore makers, followed by compaction and sintering at 1050°C. The chemical composition of the MBCP ceramic was analyzed using X-ray diffraction (XRD, Philips PW 1830 CuK $\alpha$  radiation, PW 1050 goniometer) and Fourier Transform Infrared Spectroscopy (FTIR, Nicolet, Magna-IR 550). The MBCP granules were composed of hydroxyapatite/ $\beta$ -tricalcium phosphate in a 60/40 weight ratio. The micro- and macro- porosity were measured by mercury intrusion porosimeter (AutoPoreIII, Micromeritics) and scanning electron microscopy (SEM, Leo 1450VP, Zeiss, Germany). The total porosity of the MBCP was approximately 65–70% with macropores in the 260–550  $\mu$ m size range. The microporosity was approximately 30–35% and corresponded to micropores of less than 10  $\mu$ m in size. The MBCP granules (1 g) were packaged into a glass vial and sterilized by  $\gamma$  radiation (>25 kGy). The specific surface area of the MBCP was determined using the Brunauer-Emmett-Teller (BET) method with helium adsorption-desorption (Micromeritics).

The MBCP granules were mixed with fibrin glue (Tissucol<sup>™</sup> Baxter BioSciences BioSurgery, Vienna, Austria) using a granules/fibrin glue volume ratio of 1:1 and 1:2 for the intramuscular and intrafemoral experiments, respectively. Typically, granules were humidified with 1.5 ml of sterile physiological water and then mixed with fibrin glue. The fibrin glue was packaged in a frozen kit with two syringes. The first syringe contained fibrinogen, fibronectin and factor XIII with aprotinin. The second syringe contained 4 IU of thrombin with CaCl<sub>2</sub>. Prior to use, the fibrin glue kit was thawed at 37°C for 30 min. Before mixing with fibrin glue, the MBCP granules were hydrated with sterile physiological solution. The products contained in the two syringes were simultaneously or sequentially injected onto the ceramic granules. For the sequential mixing, the syringe with thrombin was first injected onto the granules and then, the syringe containing fibrinogen was added. Regardless of the mixing method used (direct or sequential), the association led to the formation of fibrin glue on and between the ceramic granules.

The MBCP/fibrin glue composites were quantitatively and qualitatively analysed. Ten samples were prepared for each method of association. The cross-linking time was determined visually as the onset of clotting formation indicated by the opacity of the fibrin glue. For SEM observation, the

samples were dried by the CO<sub>2</sub> critical point method (CPD 010, Balzers Union, Liechtenstein). For the CPD, the samples were fixed in a glutaraldehyde solution at 3% for 20 min, then rinsed three times with cacodylate buffer, and dehydration was performed using graded ethanol series (24 h for each grade), followed by pure acetone for 48 h. Prior to the SEM observations, the blocks were coated with gold-palladium at 20 mA for 4 min (EM Scope, UK). The porosity of the reticulated MBCP/fibrin glue composite was measured in triplicate by X-ray micro-computed tomography ( $\mu$ CT, SkyScan 1072, Belgium) using 20 kV and 100 mA. Fibre thickness in the fibrin glue was determined by SEM (Leo 1450VP, Zeiss, Germany) using back-scattered electrons (BSE) at 15 kV. Five SEM images per sample ( $n = 3$ /group) were taken and thickness of 10 fibres in each image were measured using a calibrated image analysis system (Leica Quantimeter 5501W, Japan). The anisotropy depended on the orientation of fibres in the fibrin glue. It was determined as previously using SEM images and image analysis. The anisotropy index was defined as the horizontal intercept divided by vertical intercept. Horizontal and vertical fibres had an anisotropy index of 0 and 50, respectively. Intermediate values corresponded to highly anisotropic material.

## 2.2 Surgical procedure, preparation of the composite and implantation

All animal handling and surgical procedures were conducted according to the European Community guidelines for the care and use of laboratory animals (DE 86/609/CEE). The study protocol was approved by the ethics committee of the National Veterinary School in Nantes. Six adult female sheep with an average weight of 64 kg and forty-two female New Zealand White rabbits (age: 15 weeks, body weight: 3.25–3.5 kg) purchased from a professional breeder (Charles River Laboratories, L'Arbresle, France) were used in this study. Sheep intramuscular implantation were performed under general anaesthesia induced with intravenous diazepam (1 mg/kg) and ketamine (8 mg/kg) and followed by volatile anaesthesia with oxygen and halothane. During surgery, the animals received an intravenous saline isotonic solution (NaCl 0.9%) and 1 g of amoxicillin through a catheter in the jugular vein. Rabbits underwent surgery under general anaesthesia performed with intramuscular injections of xylazine (5 mg/kg, Rompun<sup>®</sup>, Laboratoire Bayer Pharma, Puteaux, France) and ketamine (35 mg/kg, Imalgène 1000<sup>®</sup>, Merial, Lyon, France). For the intramuscular implantation, each sheep received one implant bilaterally in the erector spinae muscles (*luggissimus lumborum*). Two skin and muscle incisions were made on each side of the spine, approximately 5 cm from the median axis of the spine. After incision of the skin and muscular fascia, the lumbar muscles were separated

to provide an intramuscular space with a cranio-caudal direction parallel to the spinal axis. The extremity of the syringe containing the MBCP/fibrin sealant composite was cut and the excess fibrin sealant removed. About 2–3 cm<sup>3</sup> of composite biomaterials were implanted into lumbar muscles. After implantation of the materials, the wound and skin flaps were immediately closed in two layers using resorbable sutures (Vicryl<sup>®</sup> 4–0, Johnson & Johnson Intl). After surgery, the animals received one antibiotic (amoxicillin, i.v. injection 2 g/day) for 5 days and clinical follow-up was performed during the first postoperative week. The sheep were housed in stables with unlimited food and water. Twenty-four weeks after surgery, the animals were euthanized by intravenous injection of a lethal dose of pentobarbital (Dolethal<sup>®</sup>, Vetoquinol, Lure, France). For the bone implantation, a longitudinal skin incision was made to expose the distal lateral femoral condyle. A cylindrical defect 6 mm in diameter and 10 mm deep was created at the epiphyseo-metaphyseal junction by using a motor-driven driller (Aesculap, Tuttlingen, Germany). The drilling process was completed in 3 successive steps using burs of 2, 4, and 6 mm in diameter. During the drilling process, the defect site was continuously irrigated using a syringe of sterile saline solution. The defects were then packed with sterile swabs until the bleeding had subsided. The bone defect was drilled in the centre of the lateral condyle. The defects were filled with the three different composite materials. Voids or dead spaces in the defect were minimized. The composites consisted of (i) the direct mixing group, namely the simultaneous application of the components of fibrin glue with MBCP or (ii) the sequential mixing group, corresponding to the addition of thrombin to the MBCP and subsequent addition of fibrinogen. The cavity was finally closed with an MBCP ceramic plug 6 mm in diameter and 3 mm in length. The wound was sutured in three layers (Vicryl 3–0, Ethicon, Johnson & Johnson Intl.). The rabbits were operated on bilaterally. The rabbits were housed in individual boxes with unlimited food and water. Under general anaesthesia, the 42 rabbits were euthanized by intracardiac injection of barbiturate (Dolethal<sup>®</sup>, Vetoquinol, France) at 3, 6, 12 and 24 weeks following implantation. The femoral condyles were harvested and the peripheral soft tissue removed. The samples selected for the microindentation test were directly frozen and conserved at –20°C. The other samples were fixed in neutral buffered formalin solution for 7 days, rinsed in water, dehydrated in ethanol of increasing concentration (from 70 to 100%) and then in pure acetone for 48 h. For statistical analysis, each group consisted of 6 implants. Three rabbits per group and per time were used for histology and histomorphometry. Six rabbits were used for microindentation testing at 6 weeks for the groups composed of direct and sequential MBCP/fibrin mixing.

### 2.3 Mechanical testing of the bone-filled defects

The mechanical properties of the bone-filled defects were measured with micro-indentation testing. This non-destructive technique made it possible to perform further histological and histomorphometrical analyses on the samples after the test. The bone specimens were frozen at  $-20^{\circ}\text{C}$  without fixation. The femoral epiphyses were cut in half along the axis of the femur in the middle of the trochlea using an Isomet diamond saw (Buehler LTD, Germany). The two halves showed the circular defect in the cortico-spongious bone. The samples were progressively unfrozen for 2 h. Both the spongious bone surfaces and circular defects filled with composite materials were then submitted to micro-indentation tests. The samples were kept wet during the whole mechanical analysis. Micro-indentation tests were carried out on a computer-controlled micro-indentation device (Fisherscope H100, Fisher, USA) equipped with a Vickers diamond indenter. In this work, ten tests at 100 mN maximum load were performed on each sample. The hardness tests consisted in a loading stage followed by a 20 s holding period (creep) at the maximum load and an unloading stage down to 0.4 mN. This load was then maintained for another creep period of 20 s. For each sample, five tests were performed on the trabecular bone surface and five tests on the implant. For each test, the load, penetration depth and hardness were monitored.

### 2.4 Histological and histomorphometrical analysis

The samples were soaked for 5 days in methyl methacrylate (Prolabo) and embedded in polymethylmethacrylate (PMMA) resin. Blocks were cut in order to eliminate excess PMMA and analyzed by X-ray micro-computed tomography ( $\mu\text{CT}$ , SkyScan 1072, Belgium). The X-ray source was operated at a voltage of 100 kV and current of 98  $\mu\text{A}$ . The samples were rotated through  $180^{\circ}$  with a rotation step of  $0.90^{\circ}$ , an acquisition time of 5.6 s per scan and a pixel size of 11.8  $\mu\text{m}$ . Three-dimensional reconstructions were then performed using the software 3D Creator SkyScan. The region of interest (ROI) was defined inside the limit of the defects. The volume of ceramic material, mineralized bone and empty space were then measured using X-ray micro-computed tomography ( $\mu\text{CT}$ ). The  $\mu\text{CT}$  produced a 3 dimensional image of the MBCP ceramic granules and mineralized bone inside the femoral defect. The ceramic granules and mineralized bone were distinguished on the basis of their respective gray levels. The corresponding volumes were measured and averaged. The percentage of bone was calculated by dividing the volume of bone by the available space in the defect. The available space corresponded to the total volume of defect

minus the volume of ceramic. For the ostéoinduction experiment, the number (Tb.N) and thickness (Tb.Th) of the bone trabeculae were measured in the sample. The same data were determined in the trabecular bone taken from the vertebrae of the same sheep. All specimens were then radiographed to localize the bone defect. Each block was transversally cut in the middle of the bone defect with a circular diamond saw (Leica, saw microtome 1600, Germany). For each implant, a section of 100  $\mu\text{m}$  in thickness was made with a diamond circular saw (Isomet<sup>®</sup>, Buehler LTD, Lake Bluff, USA). This section was used for bone-labelling. One part was processed for histology while the other was used for SEM histomorphometry. Thin sections (7  $\mu\text{m}$  in thickness) were then prepared using a hard tissue microtome (Reichert-Jung, Supercut 2050, Germany). The thin sections were stained with Movat's pentachrome. This stain contained alcian blue, Weighert's iron hematoxylin, brilliant crocein, acid fushin and saffron. The nuclei were stained greyish black, collagen fibres and mineralized bone were coloured in yellow. The cartilage tissue appeared in green while osteoid was coloured in red. Pictures were taken using a light microscope (Zeiss, Axioplan 2, Germany) at the magnification  $\times 100$ . The other part of the blocks was used for SEM histomorphometrical measurements. The cross-sectioned PMMA blocks were polished and sputter-coated with gold-palladium at 20 mA for 4 min (EM Scope, UK). The surfaces of the blocks were observed by scanning electron microscopy (Leo 1450VP, Zeiss, Germany) using back-scattered electrons (BSE) at 15 kV. Contiguous images were automatically taken at the same magnification of  $\times 35$ . The entire bone defect was reconstructed with 9 to 16 continuous images. Quantification was performed on these reconstructed pictures using a semi-automatic image analysis system (Leica Quantimeter 5501W, Japan). The ROI was defined as the outer limit of the circular defect. The surfaces of mineralized bone, ceramic and empty space were distinguished based on their respective grey levels and measured. The quantity of bone was expressed as a percentage by dividing the surface of bone by the empty surface. As before, the empty surface was defined as the surface available for bone growth and thus corresponded to the total circular defect minus the ceramic surface.

### 2.5 Bone-labelling

Two series of oxytetracycline injections (Terramycine 50 at 2%, Pfizer, Paris, France) were given to the first group of 36 rabbits. Fluorochromes were first injected 15 and 14 days and then 5 and 4 days before euthanasia. Intramuscular injections were given at 30 mg/kg. Two parallel fluorescent lines corresponding to the two injections of fluorochrome were observed with fluorescent light microscopy (Leica DM

RXA, Leica<sup>®</sup>, Switzerland). The measurements were performed at the same magnification of x20. The images were recorded using a CCD video camera (CCD-IRIS, SONY<sup>®</sup>, Japan) and transferred to an image analysis system (Q550 MW, Leica<sup>®</sup>, Switzerland). The image analysis system was calibrated beforehand at a magnification of x20 with a graduated scale (Stage-micrometer B-0550, 4004-602, Spectra-Tech, Inc.). For each histological section, 5 sites of double labelling were selected. On each site, five measurements were taken and averaged in order to limit experimental errors resulting from different cutting angles according to the original Frost's procedure. The averaged distances were then divided by the number of days (10 days) between the two injections. The bone growth rate was obtained in micrometers per day [26].

### 2.6 Statistical analysis

All data were expressed as mean and standard deviation. The differences were evaluated with variance analysis (ANOVA) with Fisher's probability test significant difference (PLSD) post hoc test. The differences were considered to be significant at  $p < 0.05$ .

## 3 Results

### 3.1 Characterization of implant materials

The chemical, physical, biological and ultra structural properties of the MBCP/fibrin composite are summarizing in Table 1. SEM images of the structure MBCP, fibrin glue and MBCP/fibrin glue composite material are shown in Fig. 1. The MBCP granules have both macro- and micro-porosity in the 100–600 and  $<10 \mu\text{m}$  range respectively (Fig. 1(a)). The polymerization of the fibrin glue formed a complex network of fibres shown in Fig. 1(b). The fibrin glue partially covered the surface and penetrated the microstructure of the ceramic material as well as providing cement between the ceramic granules (Fig. 1(c)). The fibrin clot was heterogeneous, with dense and narrowed mesh regions. Direct or sequential mixing of the fibrin glue with the MBCP ceramic demonstrated a similar microstructure of the composite material (data not shown). After mixing, the MBCP/fibrin composites were used for implantation into muscles of sheep and for filling critical sized bone defect in the femoral condyle of rabbits. Figure 1(d) shows a three dimensional reconstruction using  $\mu\text{CT}$  technique of MBCP/fibrin implants after intramuscular implantation for 24 weeks. In the 3D image, the

**Table 1** Chemical, physical, biological and ultra structural properties of MBCP granules, fibrin glue and MBCP/fibrin glue composite material

Chemical composition				
	HA (%wt) <sup>(1)</sup>	$\beta$ -TCP (%wt) <sup>(1)</sup>	Ca/P <sup>(1)</sup>	Specific surface area (m <sup>2</sup> /g) <sup>(2)</sup>
MBCP	60 ± 2	40 ± 2	1.60 ± 0.02	1.8 ± 0.1
Physical properties				
	Size of granules (mm)	Total porosity (%) <sup>(3)</sup>	Size of macropore <sup>(3)</sup> ( $\mu\text{m}$ )	Size of micropore <sup>(3)</sup> ( $\mu\text{m}$ )
MBCP	1–2	70	450 ± 49	0.43 ± 0.2
Biological composition				
	Fibrinogen concentration (mg/ml)	Thrombin concentration (UI)	Global porosity (%)	Reticulation time (s)
Fibrin glue	100	4	60	60
Ultra structural properties				
	Anisotropy <sup>(4)</sup>	Density <sup>(4)</sup>	Pore size <sup>(4)</sup>	Thickness of the fibers ( $\mu\text{m}$ ) <sup>(4)</sup>
MBCP/fibrin glue composite	Average*	Very low*	0.7 ± 0.06	0.10 ± 0.04

<sup>(1)</sup> Analyzed by XRD;

<sup>(2)</sup> Analyzed by BET;

<sup>(3)</sup> Analyzed by Hg porosimetry;

<sup>(4)</sup> Analyzed by SEM with image analysis;

\*Comparing to MBCP/fibrin glue composite with 500 or 50 UI of thrombin.

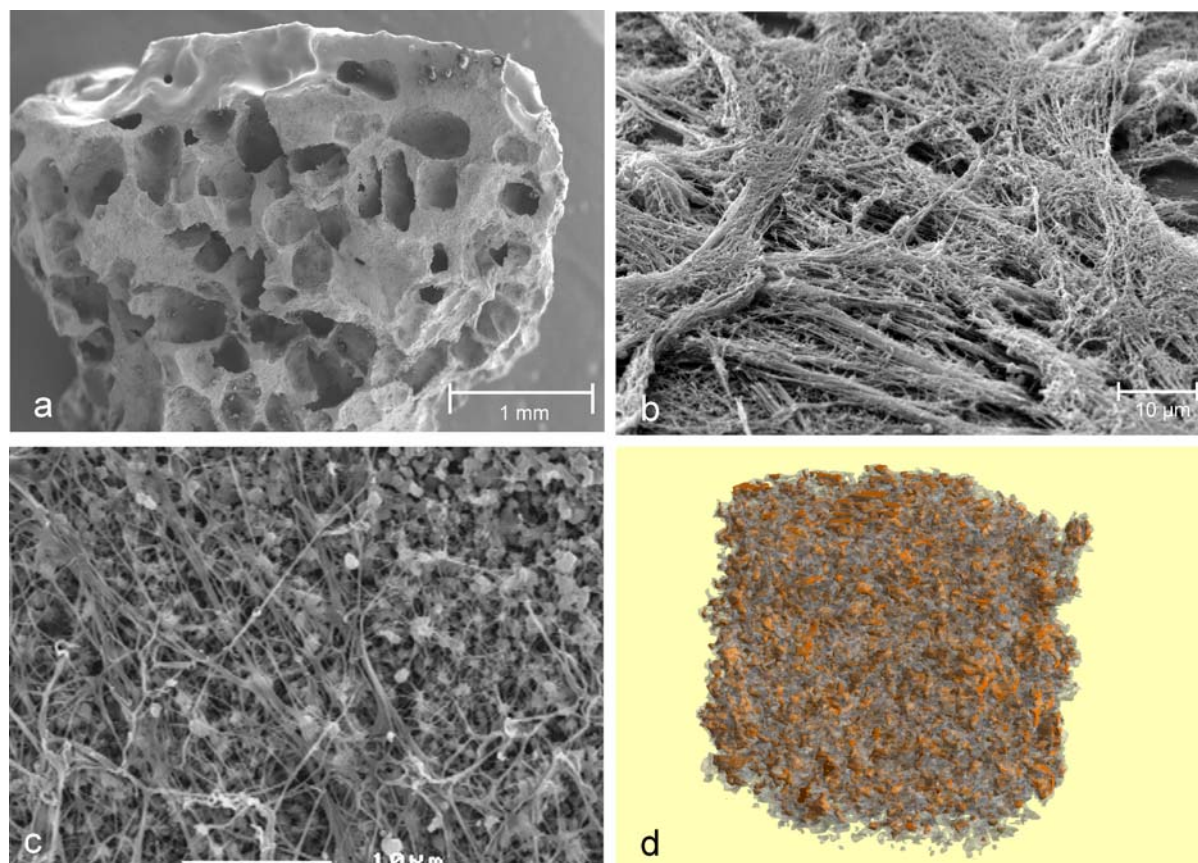


**Fig. 1** SEM micrographs of the MBCP granules (a) showing a macro-micro-porous surface and the fibrin clot formed alone (b) or on the MBCP granules (c). Note the fibrin fibers penetrating the micro-porous surface. Micro-computed tomography global view image (d) of

MBCP/fibrin implants after intramuscular implantation for 24 weeks in sheep back muscles. Orange: MBCP granules, grey: bone and yellow: muscle tissue

MBCP ceramic granules appeared in orange while the mineralized bone was in light gray depending on their respective X-ray absorbance. Superposition of mineralized bone and ceramic gave a brown color.

### 3.2 Histological and histomorphometrical observations

In intramuscular sites of sheep, histological sections of the MBCP/fibrin implants show newly formed bone using both polarized light microscopy and Movat's pentachrome staining (Fig. 2). Organized collagen fibers with abundant osteocytes and osteonal systems were clearly visible between the MBCP granules by using polarized light (Fig. 2(a)). Mineralized and mature bone tissue was in direct contact and bridged the MBCP granules. The ectopic bone was surrounded by muscle tissue (Fig. 2(b)). Back scattered electron micrographs of the MBCP/fibrin material are shown in Fig. 3. Only the MBCP ceramic granules and mineralized bone were noticeable. These two structures can easily be distinguished by their grey levels and morphology. Newly formed bone was not homogeneous but limited to the implantation site (Fig. 3(a)). Bone tissue was well mineralized with numerous

lacunae. Ectopic bone formation appeared in direct contact to the ceramic granules and was observed inside and between the calcium phosphate particles (Fig. 3(b)).

In critical sized bone defect of rabbits, the bone ingrowth was observed using histology and SEM for the two different materials after 3, 6, 12 and 24 weeks of implantation (Fig. 4). For both group, MBCP/fibrin direct mixing (Figs. 4(a)–(d)) and MBCP/fibrin sequential mixing (Figs. 4(e)–(h)), the MBCP ceramic granules appeared in light gray and mineralized bone being more greyish. For the two groups, the bone defects filled with the composite materials, showed mineralized bone tissue growing centripetally in between the ceramic granules. Newly formed bone tissue was in direct contact with the MBCP granules. These SEM observations demonstrated the osteoconductive properties of the two composite materials prepared by the direct or sequential methods. With increasing implantation time, the quantity of mineralized tissue appeared to be more abundant. Movat's pentachrome staining corroborated bone tissue apposition previously observed at the surface of the MBCP granules with SEM. After 3 weeks of implantation, the calcium phosphate ceramic granules were homogeneously distributed over

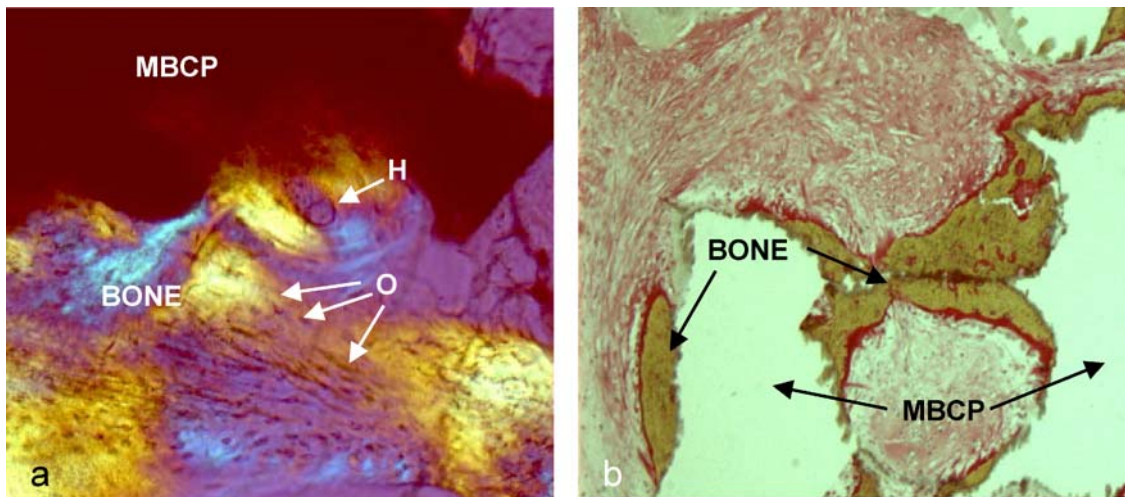


**Fig. 2** Histology pictures of MBCP granules with fibrin glue after intramuscular implantation for 24 weeks in sheep back muscles. (a) Polarized light images showing mineralized bone with osteocytes (O) and

Haversian (H) structures formed between the MBCP granules. (b) Histological images showing a bone trabecula between the MBCP granules (Movat's pentachrome stain)

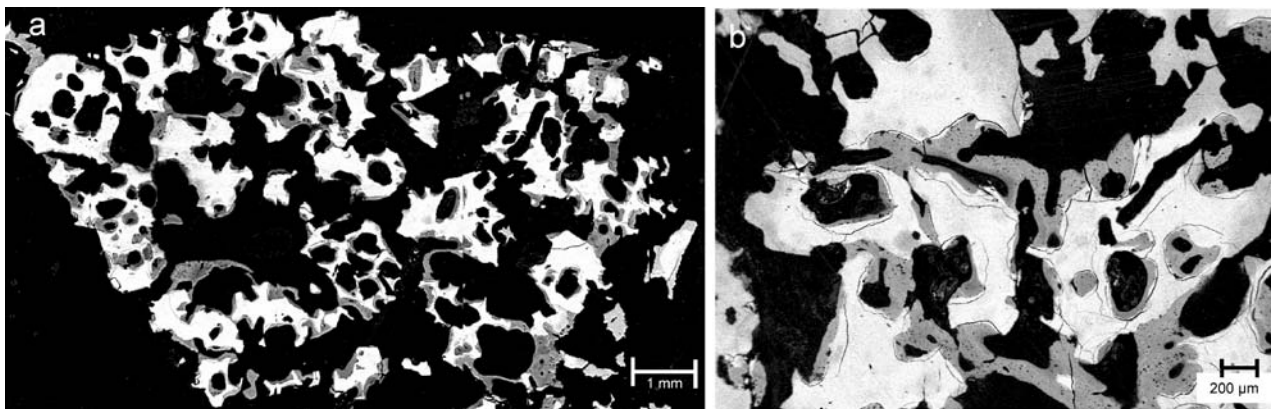


**Fig. 3** BSE images of MBCP granules after intramuscular implantation for 24 weeks into the back muscles of sheep. Note ectopic bone trabeculae formed between the MBCP granules and inside the macropores (a)

and the formation of well mineralized bone with osteocytes (b) White: MBCP granules, grey: bone, black: muscle tissue

the bone defect. At this early stage, newly formed bone was observed in the groups with an osteoid layer. After 6 weeks, the sections showed a homogenous mineralized tissue over the implantation site with most bone formation than after 3 weeks of implantation (data not shown).

### 3.3 Quantitative bone analysis

After 24 weeks of implantation into muscles of sheep, histomorphometrical analysis was performed for the MBCP/fibrin implants using two methods, SEM and  $\mu$ CT. The BSE method gave a percentage of bone significantly lower than the  $\mu$ CT method for the composite implants,  $6.7 \pm 3.7$  and  $17.0 \pm 2.2$ , respectively. The X-ray microtomography technique provided with the number of trabeculae (NTb,  $15.6 \pm 3.2 \times 10^{-3} \mu\text{m}^{-1}$ ) and thickness of the trabeculae ( $216 \pm 32 \mu\text{m}$ ) for the ectopic bone formed in the

MBCP/fibrin implants. These data were similar to the number ( $16.1 \pm 3.6 \times 10^{-3} \mu\text{m}^{-1}$ ) and thickness ( $278 \pm 40 \mu\text{m}$ ) of the trabeculae measured in the trabecular bone of the vertebral body ( $p < 0.01$ ).

Figure 5 shows the percentage of bone growth in the critical sized defects determined by the two histomorphometrical methods, SEM and  $\mu$ CT, in relation to materials and implantation time. The SEM and image analysis method provided with a two dimensional quantification of bone growth while  $\mu$ CT gave a volumetric measurement. Regardless of which method was used, the quantity of bone increased with implantation time in both groups. The amount of bone was lower at 3–6 weeks than at 12–24 weeks of implantation ( $p < 0.05$ ). This difference in bone growth might be related to bone healing and remodelling in the early stages. For the MBCP/fibrin direct mixing group, the quantity of bone increased similarly with implantation time regardless of measurement method.

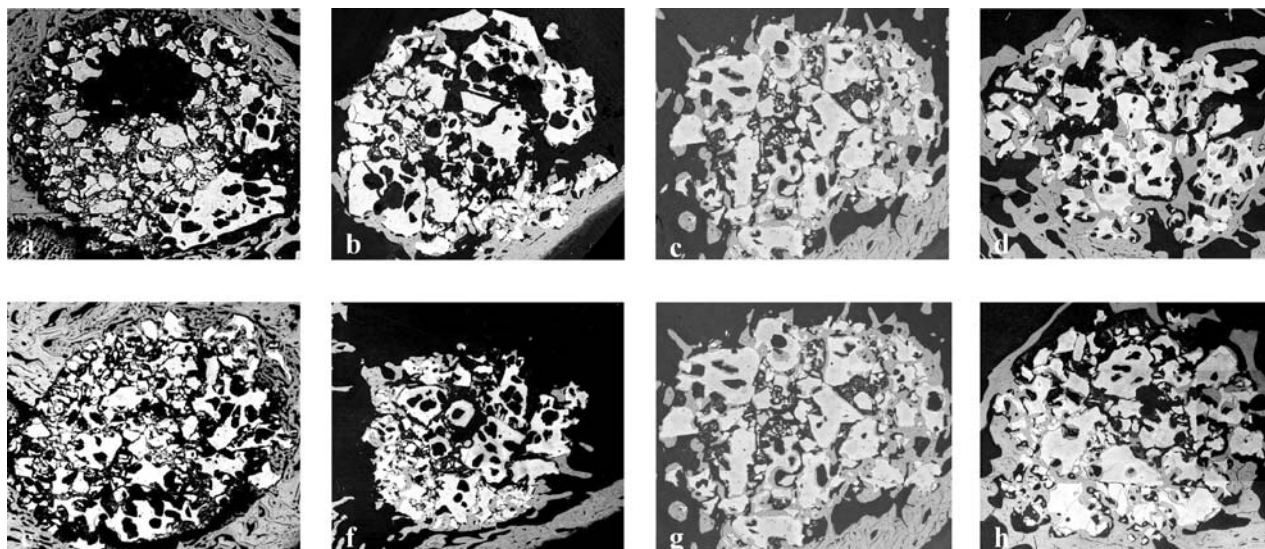


**Fig. 4** BSE micrographs of the different MBCP/fibrin materials after 3(a, e), 6(b, f), 12(c, g) and 24(d, h) weeks of implantation. The MBCP/fibrin direct mixing group (a, b, c, d) and MBCP/fibrin sequen-

tial mixing group (e, f, g, h). Newly bone was formed between the MBCP granules from the edge towards the centre of the defect. (White: MBCP granules, gray: bone and black: connective tissue)

**Fig. 5** Bone growth in the two different materials after 3, 6, 12 and 24 weeks of implantation into critical sized defects in the femoral epiphysis of rabbits. For the SEM technique, bone growth was expressed as a percentage by dividing the surface of the bone by the surface of the empty space. For the  $\mu$ CT technique, the percentage of bone was obtained by dividing the volume of bone by the empty volume

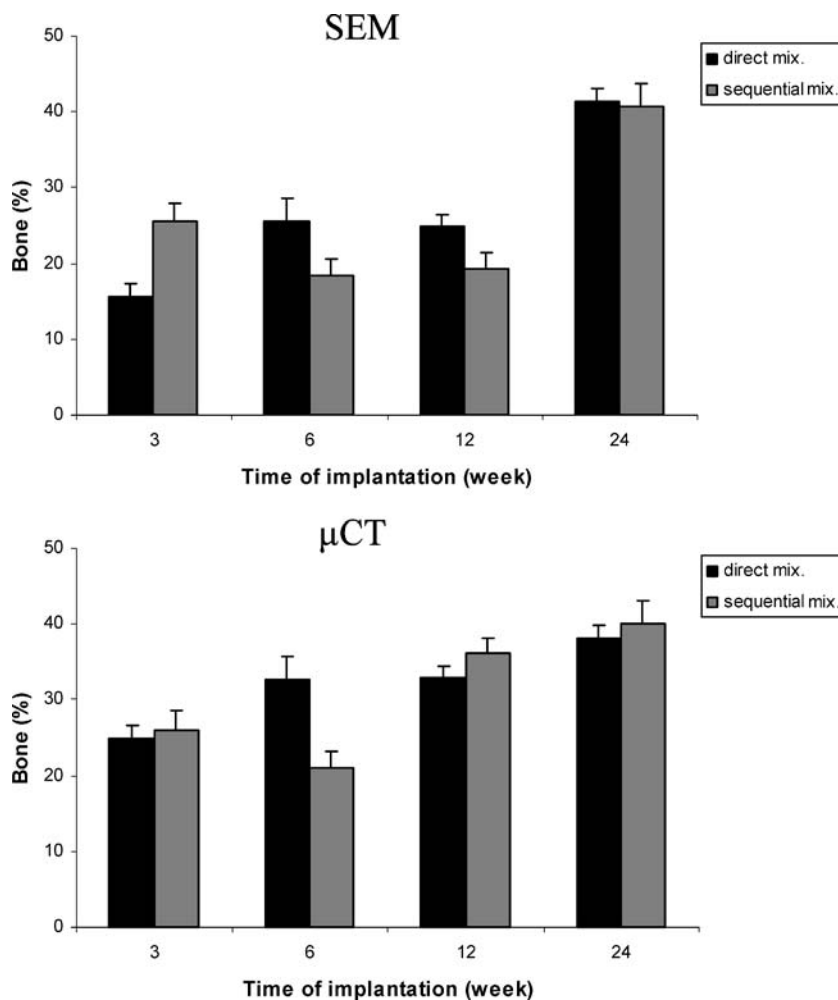




**Table 2** Micro indentation testing of the different MBCP/fibrin materials after implantation for 6 weeks in rabbit femoral epiphyses. Mechanical testing of trabecular bone was used for comparison

Materials	Penetration depth ( $\mu\text{m}$ )	Hardness ( $\text{N}/\text{mm}^2$ )
Trabecular bone ( $n = 40$ )	$4.8 \pm 0.9$	$180.7 \pm 64$
MBCP/fibrin (direct mix.) ( $n = 20$ )	$9.7 \pm 2.4$	$118.6 \pm 60.6$
MBCP/fibrin (sequential mix.) ( $n = 20$ )	$53.6 \pm 11.4$	$2 \pm 1.1$

After initial growth, a plateau was reached at 6–12 weeks and the quantity of bone increased again at 24 weeks. In the case of the MBCP/fibrin sequential mixing group, the bone growth was initially greater at 3 weeks than at 6 weeks. After 12 and 24 weeks, the quantity of bone measured by the two methods was higher than at 6 weeks.

The bone labelling was performed to determine the bone growth rate. Two injections of oxytetracycline at 10 day intervals prior to euthanasia allowed the observation of the mineralized fronts under fluorescent microscopy. The distance between this two fronts lines divided by the number of day between the two injections is equivalent to the bone growth rate. For both groups and all the implantation time, the bone growth rates were between 1.5 to 2.1  $\mu\text{m}/\text{day}$ . After 3 weeks, the sequential mixing preparation gave the most important growth rate. Nevertheless, after implantation for 12 and 24 weeks, the sequential mixing group gave again the highest rate of bone growth (data not shown). These values were comparable to previously published data giving 1.9  $\pm$  0.3  $\mu\text{m}/\text{day}$  in rabbit femurs [27].

Table 2 shows the results of micro-indentation tests performed on the two composite materials after 6 weeks of implantation, comparing to the surrounding trabecular bone. In agreement with previously published data, the trabecular host bone exhibited a hardness of  $180.7 \pm 64.1 \text{ N}/\text{mm}^2$  and a Young's modulus of  $7.4 \pm 2.2 \text{ GPa}$  [28]. The values obtained for the MBCP/fibrin direct mixing group were slightly lower but significantly lower for the MBCP/fibrin sequential mixing group.

#### 4 Discussion

Calcium phosphate ceramic are widely used in the reconstruction of bone defects. Many studies have shown their bioactivity and osteoconductive properties. Nevertheless, these synthetic materials generally lack osteogenic properties to regenerate bone tissue over large or critical sized bone defect [29]. Moreover, bioceramics in the form of blocks or granules are not easy to handle and to maintain in the surgical sites while empty spaces between bone tissue and filling material are often present. The addition of fibrin glue provides with a biological liquid matrix that forms a gel around the ceramic granules to fit the anatomy of the bone defects [30]. In this study, we have associated fibrin glue to a bioceramic to

improve the mouldable and osteogenic properties of the synthetic material. Due to the setting time of the fibrin (around 10 min), the composite materials were easily placed whether in the paravertebral muscles of sheep or in the femoral defect of the rabbit. Osteogenic properties of materials are described by both osteoconductive and osteoinductive properties [8–10, 31, 32]. Osteoinduction by materials is a complex phenomenon, not yet fully understood and being both material- and animal-dependant.

In our study, a composite made of MBCP granules and fibrin glue induced both ectopic bone formation in sheep muscles and bone healing in critical sized defects in rabbit femurs. Ectopic bone formation was observed in direct contact to the granules, inside the macropores and bridging the particles forming trabeculae. Newly formed bone appeared well-mineralized, containing osteocytes and exhibiting Haversian structures. The quantity of ectopic bone was about 6.7% with BSEM method and 17% with  $\mu\text{CT}$  method. The number and thickness of the bone trabeculae were comparable with those measured in spongy bone in the same animal. The fibrin glue is well known for its properties regarding cell attraction, proliferation and differentiation in the wound healing process [15, 33]. Despite all these biological properties, the osteoinductive potential of fibrin glue is not clearly understood. After intramuscular implantation for 24 weeks, mineralized bone tissue, neither exhibited cartilage tissue nor chondrocytes. The newly formed bone inside the MBCP/fibrin material had probably followed the route of intramembranous ossification [36]. Surface microstructure of the bioceramics plays a key role in bone formation and healing [11]. Bone formation may be due to an inflammatory reaction produce by the local release of micro particles from the surface of the biomaterial [37]. The degradation of the blood clot within a bone fracture might also provoke a local inflammatory reaction. In our study, the fibrin glue mixed with bioceramics might also provoke a local inflammatory reaction which promotes the proliferation and differentiation of mesenchymal stem cells to form bone tissue [38]. Vascularization is also considered to be a crucial step in osteogenesis. Several studies have reported the benefits of fibrin glue onto wound healing and even osteogenesis [39, 40]. In the present study, blood vessels were observed both macroscopically and histologically (data not shown). The blood vessels were observed in between the MBCP ceramic granules and near mineralized bone tissue. Nevertheless the results of these works have not

made it possible to draw conclusions about the effect of fibrin glue on bone formation in ectopic sites. In fact, the fibrin clot degraded within two weeks whereas newly formed bone is usually observed after 6–12 weeks in muscles [22, 41]. Fibrin glue component (fibrinogen, thrombin, fibronectin) may act just after implantation in the early stage of ectopic bone formation [42]. The fibrin glue also form a similar blood clot as it observed after a bone fracture. Degradation of this clot generally occurred in a few days [34]. The products of degradation and the macrophagic cells involved in this pathway allow the recruitment of many cell populations, like osteoprogenitor cells, in the bone fracture site. A neo vascularisation process occurred in the bone defect while an abundant extra cellular matrix is produced by the osteoblastic cells and mineralized in a second time. This woven bone is involved in the process of bone turn over and remodelled by the synergistic action of osteoblastic and osteoclastic cells according to the Wolff's law [35]. With these MBCP/fibrin composites, we attempted to induce bone formation in the muscle of sheep and to mimic the bone healing process of fractures.

In the rabbit experiment, combination between fibrin glue and bioceramic was performed whether by direct mixing or by a sequential application of the fibrin glue component. These two associations aimed to show the influence of the adsorption of thrombin onto the MBCP granules on the mechanical and osteogenic properties of the composite material. Bone healing was observed after implantation of both materials in a rabbit bone defect. As shown in Fig. 5, for both materials, after an initial bone growth, the quantity of newly formed bone reached a plateau and finally increased. The plateau may correspond to the period of remodelling process occurred between 3 and 12 weeks. Slight differences are observed in bone quantity with implantation time between the materials. Bone remodelling process seems to be observed after 6 weeks of implantation, the group of MBCP/fibrin glue mixed sequentially while MBCP/fibrin direct mixing material produced later bone remodelling, between 6 and 12 weeks. These differences in the bone healing process can be explained by the different osteogenic properties of each composite material. This delay may also explain the difference in mechanical strength observed for the two composite materials after 6 weeks of implantation (Table 2). At this time, The MBCP/fibrin glue direct mixing material exhibits a better mechanical strength than the sequential one. A good correlation was therefore observed between the quantity of bone and the mechanical strength in the material-filled femoral defects. The difference of mechanical strength between these two composite materials could be also explained by their mode of preparation: direct or sequential mixing method. In the first process, the three main components of the composite material, fibrinogen, thrombin and MBCP granules, were simultaneously mixed. In the second one, thrombin component was first adsorbed onto the surface of MBCP granules

and then mixed with fibrinogen. Qualitatively, we noticed that the direct mixing provided better initial strength for the MBCP/fibrin glue composites than the sequential mixing. The direct mixing association of the three components may lead to the formation of a 3 dimensional network of fibrin fibres in which the granules are fully incorporated. By using the sequential mixing association, the network formation appeared with different biophysical properties. The network may be weaker with diffuse fibres into the composite than for the direct mixing method.

## 5 Conclusion

The osteogenic property of MBCP/fibrin glue composite materials was studied using two animal models, intramuscularly in sheep and intraosseously in rabbits using a critical sized bone defect. Bone tissue had formed ectopically in contact with the surface of the ceramic after 24 weeks. The newly formed bone appeared well-mineralized, forming trabeculae between the granules, and had characteristics similar to those of cancellous bone. Bone growth in the femoral defects of rabbits filled with the MBCP/fibrin materials increased with implantation time. The newly formed bone was in direct contact with the MBCP granules and progressed centripetally. The sequential mixing of the fibrin components seemed to initiate an early bone remodelling but resulted in poor mechanical properties for the bone defect filled with the MBCP/fibrin glue composite. In summary, these MBCP/fibrin composite materials exhibited interesting biological and mechanical properties for filling large bone defect. These composites may also be used in combination of bone marrow cells for bone tissue engineering applications.

**Acknowledgments** This study was supported financially by both the "Réseau National des Technologies pour la Santé" (RNTS 2002) and the "Contrat Etat Région" (CER Biomaterials 2000–2006). The authors would like to thank Baxter Bioscience for providing the fibrin glue (Tissel, Baxter BioScience, BioSurgery, Vienna, Austria) and Biomatlante France, manufacturer for the biphasic calcium phosphate (TricOs<sup>®</sup>, Baxter BioSciences BioSurgery). We also acknowledge M. Tanguy Honore from the Centre de Transfert de Technologie du Mans for his technical expertise in the micro indentation testing.

## References

1. R. LANGER and J. P. VACANTI, *Science* **260**(5110) (1993) 920.
2. H. BURCHARDT, *Orthop. Clin. North. Am.* **18**(2) (1987) 187.
3. L. T. KURZ, S. R. GARFIN and R. E. BOOTH, JR., *Spine* **14**(12) (1989) 1324.
4. F. D. BURSTEIN et al., *Plast. Reconstr. Surg.* **105**(1) (2000) 34.
5. C. DELLOYE, *Chir. Organi. Mov.* **88**(4) (2003) 335.
6. E. J. BIEBER and M. B. WOOD, *Clin. Plast. Surg.* **13**(4) (1986) 645.

7. P. FRAYSSINET et al., *Biomaterials* **14**(6) (1993) 423.
8. G. DACULSI et al., *J. Mater. Sci. Mater. Med.* **14**(3) (2003) 195.
9. U. RIPAMONTI, J. CROOKS and A. KIRBRIDE, *South Africa J. Sci.* **95** (1999) 335.
10. H. YUAN et al., *J. Mater. Sci. Mater. Med.* **13**(12) (2002) 1271.
11. P. HABIBOVIC et al., *Biomaterials* **26**(17) (2005) 3565.
12. F. BARRERE et al., *J. Biomed. Mater. Res.* **66A**(4) (2003) 779.
13. D. M. ALBALA, *Cardiovasc. Surg.* **11** (Suppl 1) (2003) 5.
14. H. MATRAS, *J. Oral. Maxillofac. Surg.* **43**(8) (1985) 605.
15. R. R. PFISTER and C. I. SOMMERS, *Cornea* **24**(5) (2005) 593.
16. L. LE GUEHENNEC, P. LAYROLLE and G. DACULSI, *Eur. Cell. Mater.* **8** (2004) 1; discussion 1–11.
17. N. SCHWARZ, *Ann. Chir. Gynaecol. Suppl.* **207** (1993) 63.
18. S. ABIRAMAN et al., *Biomaterials* **23**(14) (2002) 3023.
19. A. R. WITTKAMPF, *J. Craniomaxillofac Surg.* **17**(4) (1989) 179.
20. G. DACULSI et al., *Ann. Otol. Rhinol. Laryngol.* **101**(8) (1992) 669.
21. R. S. SPITZER et al., *J. Biomed. Mater. Res.* **59**(4) (2002) 690.
22. W. BENSALID et al., *Biomaterials* **24**(14) (2003) 2497.
23. L. LE GUEHENNEC et al., *J. Mater. Sci. Mater. Med.* **16**(1) (2005) 29.
24. D. LE NIHOANNEN et al., *Biomaterials* **27**(13) (2006) 2716.
25. G. BLUTEAU et al., *Biomaterials* **27**(15) (2006) 2934.
26. H. M. FROST, *Calcif. Tissue Res.* **3**(3) (1969) 211.
27. L. LE GUEHENNEC et al., *J. Biomed. Mater. Res. B. Appl. Biomater.* **72**(1) (2005) 69.
28. M. RAMRAKHIANI, D. PAL and T. S. MURTY, *Acta. Anat. (Basel)* **103**(3) (1979) 358.
29. D. LE NIHOANNEN et al., *Bone* **36**(6) (2005) 1086.
30. F. JEGOUX et al., *Arch. Orthop. Trauma. Surg.* **125**(3) (2005) 153.
31. H. YAMASAKI and H. SAKAI, *Biomaterials* **13**(5) (1992) 308.
32. H. YUAN et al., *J. Mater. Sci. Mater. Med.* **9**(12) (1998) 723.
33. D. J. GEER, D. D. SWARTZ and S. T. ANDREADIS, *Tissue Eng.* **8**(5) (2002) 787.
34. G. HARASEN, *Can. Vet. J.* **43**(4) (2002) 299.
35. O. M. PEARSON and D. E. LIEBERMAN, *Am. J. Phys. Anthropol* **39**(Suppl) (2004) 63.
36. H. YUAN et al., *J. Mater. Sci.: Mat. Medi.* **9**(12) (1998) 717.
37. J. LU et al., *J. Mater. Sci. Mater. Med.* **15**(4) (2004) 361.
38. Y. YAMADA et al., *J. Craniomaxillofac. Surg.* **31**(1) (2003) 27.
39. T. R. SANTHOSH KUMAR and L. K. KRISHNAN, *Biomaterials* **22**(20) (2001) 2769.
40. J. M. KARP et al., *J. Biomed. Mater. Res. A.* **71**(1) (2004) 162.
41. P. HABIBOVIC et al., *Biomaterials* **26**(1) (2005) 23.
42. G. LI et al., *J. Orthop. Res.* **23**(1) (2005) 196.